High and Moderate-Level Vacuum Packaging of Vibratory MEMS

Igor P. Prikhodko[1,2]*, Brenton R. Simon[1]*, Gunjana Sharma[1], Sergei A. Zotov[1], Alexander A. Trusov[1], Andrei M. Shkel[1]
[1]MicroSystems Laboratory, Dept. of Mechanical and Aerospace Engineering, University of California, Irvine, CA 92697, USA
[2]Inertial MEMS and Sensors Technologies, Analog Devices Inc, 804 Woburn St, Wilmington, MA 01887, USA
Email: igor.prikhodko@analog.com, {brsimon, gunjanas, szotov, atrusov, ashkel}@uci.edu

Abstract
We report vacuum packaging procedures for low-stress die attachment and versatile hermetic sealing of resonant MEMS. The developed in-house infrastructure allows for both high and moderate-level vacuum packaging addressing the requirements of various applications. Prototypes of 100 μm silicon-on-insulator Quadruple Mass Gyroscopes (QMGs) were packaged using the developed process with and without getters. Characterization of stand-alone packaged devices with no getters resulted in stable quality factors (Q-factors) of 1000 (corresponding to 0.5 Torr vacuum level), while devices sealed with activated getters demonstrated Q-factors of 1.2 million (below 0.1 mTorr level inside the package). Due to the high Q-factors achieved in this work, we project that the QMG used in this work can potentially reach the navigation-grade performance, potentially bridging the gap between the inertial silicon MEMS and the state-of-the-art fused quartz hemispherical resonator gyroscopes.

Keywords
MEMS gyroscope, packaging, getter, quality factor.

1 Introduction

An important measure of MEMS performance is a mechanical quality-factor (Q-factor) defined as a ratio between stored and dissipated energy in a system, at the resonance frequency [1]. High quality factor is desirable for resonant MEMS (Fig. 1) as it directly translates to the improved noise resolution and higher measurement sensitivity.

Fig. 2 shows bias instability and Q-factor dependence for the state-of-the-art MEMS gyroscopes reported in open literature, demonstrating an improvement of the performance with the Q-factor increase. For instance, commercial gyroscopes employed for consumer applications often exhibit rather low Q-factors on the order of 100, and thus provide only a fraction of the degrees-per-second bias instability. In contrast, silicon gyroscopes with significantly higher Q-factors (10,000 and above) provide bias instability that is on the order of sub-degree-per-hour (1/3600 of a degree-per-second) [2]. The exception is a state-of-the-art commercial MEMS by ADI [9] with the bias instability of 4 °/hr, but the Q-value of only 50, enabled by the process integration.

Fig. 2 not only reveals the apparent trend between the Q-factors and the bias, but also shows that the state-of-the-art gyroscopes (with Q above 50 thousands) are approaching navigational grade performance [12], [3], [5]. Although not fabricated using MEMS technologies, the Hemispherical Resonator Gyroscope (HRG) currently holds the record for lowest bias stability at 10^{-4} °/hr, which is partially enabled by its exceptional Q-factor of above 10 million. The resulting Q-factor of resonant MEMS depends on the sensor design, and strongly on the pressure level of the hermetically sealed

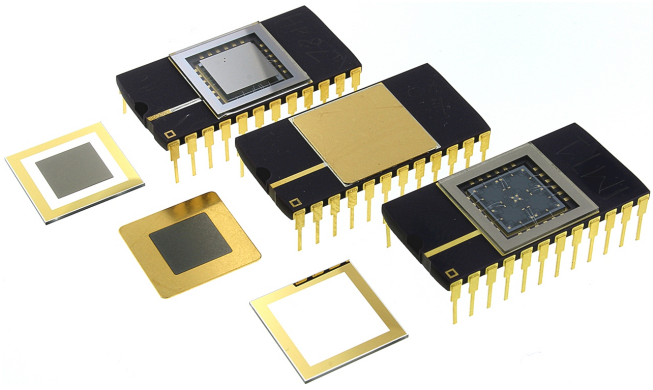

Figure 1: In-house vacuum sealed 100 μm quadruple mass gyroscopes, showing a variety of packaging options with and without getters using kovar and glass lids.

package. While MEMS gyroscopes sealed at moderate-level vacuum (0.5 Torr) provide wide bandwidth, wide linear input range, as well as reduced temperature sensitivities, the trade-off is a sacrifice in the resolution due to lower Q-factors. High Q-factors, on the other hand, are achieved at lower pressures (below 0.1 mTorr) and provide improved noise resolution. However, taking full advantage of high-Q structure and enabling sub-0.1 degree per hour rate noise performance without limiting the measurement bandwidth and linear range necessitates strict fabrication tolerances and advanced control architectures. Moreover, achieving and maintaining reliable high vacuum throughout the lifetime of the sensor requires getters for absorption of residual gases and lead to increased packaging and trim costs. The sensor application determines

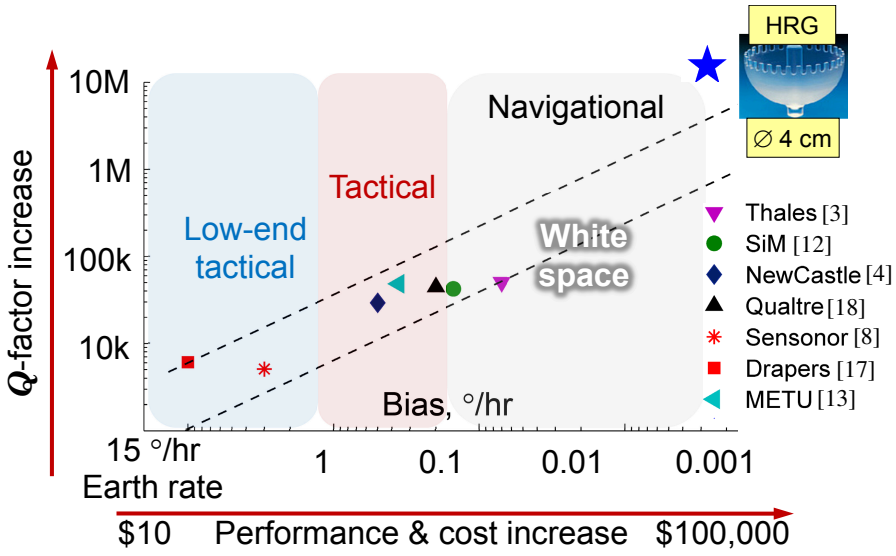

Figure 2: Q-factor and bias values for the state-of-the-art MEMS gyroscopes reported in open literature, showing improvement of the performance with the Q-factor increase.

the required Q-factors (high or moderate-level), and thus choice of a vacuum level inside the hermetically sealed packages.

Contributions of this paper compared to the prior work reported in [10], [11] is a development of the in-house infrastructure for packaging MEMS devices in controlled atmospheres or high vacuum environment, as well as the developed low-stress die attachment process. The packaging procedures were evaluated using the low-dissipation silicon MEMS Quadruple Mass Gyroscope (QMG) [16], which lead to the demonstration of Q-factors of 1.2 million [7], [21], [20], surpassing the state-of-the-art value by an order of magnitude [2]. Supported by noise analysis [15], we project that the device used in this work can potentially reach the navigation-grade performance (owing to ultra-high Q-factors), potentially bridging the gap between the inertial silicon MEMS and the fused quartz HRG.

2 Packaging Overview

The reported vacuum packaging process, developed based on the previously reported procedures from [11], is a package-level process optimized for this work by modifying the operating conditions and ensuring low-stress and void-free QMG prototypes. The packaging procedure includes two separate steps: the eutectic attachment of a micromachined die to a ceramic package, followed by the hermetic lid sealing of the package. Both steps are performed using the high temperature vacuum furnace by SST International. While the packaging recipe developed in the course of this work is described in Sections 3 to 5, here we highlight the main steps.

Due to the temperature limits of most MEMS devices, eutectic solder attachment are preferred because of its low reflow temperatures [6]. The die attachment process [11],

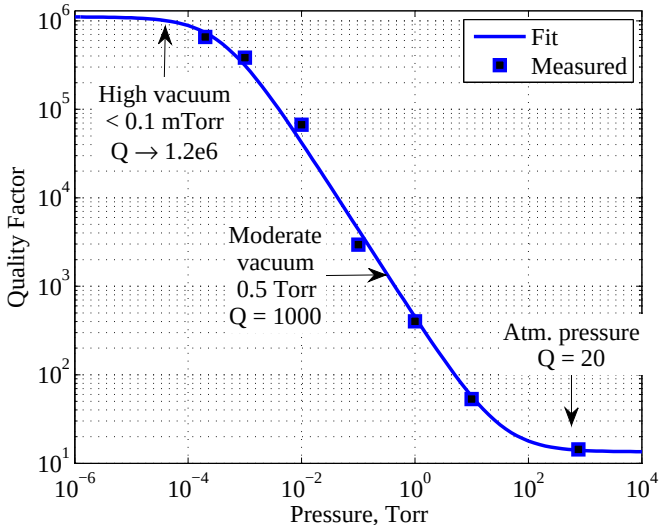

Figure 3: The measured Q-factors of the quadruple mass gyroscope as functions of pressure in a range between atmospheric (760 Torr) and 0.1 mTorr vacuum.

Section 3, uses an 80/20 gold-tin eutectic solder preform to permanently bond the gold metalized backside of a MEMS die to a gold plated ceramic package. During the die attachment process the solder is first reflowed at temperatures above the Au-Sn melting point of 278 °C, and then solidified at room temperature by active cooling. The proper reflow was done in a vacuum furnace to ensure high quality void-free bonding. In this work, the package stress is mitigated by significantly minimizing the die attachment area.

To prepare for hermetic lid sealing, a few additional steps are performed. The die attached MEMS device is wire-

bonded to the ceramic package gold pads, which provide electrical interconnects to the device. The loop heights are adjusted to ensure that wires are low enough to prevent electrical shorting. Once the die was wire bonded and inspected, a frequency characterization is typically performed to test mobility of a device. Finally, the packaged wire-bonded devices are ready for hermetic sealing.

The hermetic packaging is similar to the die attachment process, where the package lids are sealed with the eutectic solder. Kovar metal lids or custom-made glass lids are typically chosen for the hermetic sealing. For the permanent lid bonding, the preform frames of the same Au/Sn solder material are utilized. Schematics and profile of the lid sealing process flow is described in detail in Sections 4 and 5.

The sealing is performed either with or without getters (deposited on the glass lids) depending on the required level of vacuum inside the package, Fig. 3. To achieve moderate vacuum levels (above 20 mTorr), in-house lid sealing is performed. Achieving and maintaining high vacuum levels in MEMS packages (below 0.1 mTorr) requires the getter activation for absorption of gasses, which can be performed using a SST 3150 high temperature vacuum sealing furnace (now available at the UC Irvine MicroSystems Laboratory).

3 Low-Stress Die Attachment

Partial contribution of this work is the development of a low-stress die attachment process by significantly minimizing the die attachment area. While die attachment procedures are discussed in detail in [11], here we adapt this process through the use of a UniTemp RSS-160 solder reflow system.

The package surface treatment prior to die attachment is a critical step for ensuring the reliability of the stand-alone MEMS. The package surface typically contain adsorbed gasses and moisture [6], which can cause detrimental effect on resonant MEMS. The recommended method for water and surface gases removal is baking at an elevated temperature in a vacuum environment. Once trapped gases are removed and the surface condition is satisfied, the packages should be immediately sealed to avoid exposure to any gas pressure for long period of time. A proper bake out is performed at the vacuum environment (1-20 mTorr) and at temperatures up to 400 °C to facilitate outgassing and to help maintain the vacuum level in the sealed cavity.

Prior to the attachment, the vacuum chamber was also baked out for approximately 3 hours at a temperature of 250 °C. The bake-out of blank packages was performed at temperatures of up to 410 °C for a period of time no longer than 1 hour. The attachment of the QMG die to the package was facilitated by a custom-manufactured graphite locator [11], which was inserted into the gold plated cavity of the package to align components during the subsequent reflow processes. The components placed within the cavity include a 80/20 gold-tin eutectic solder preform, QMG die with a backside gold metallization layer, and a precision graphite die

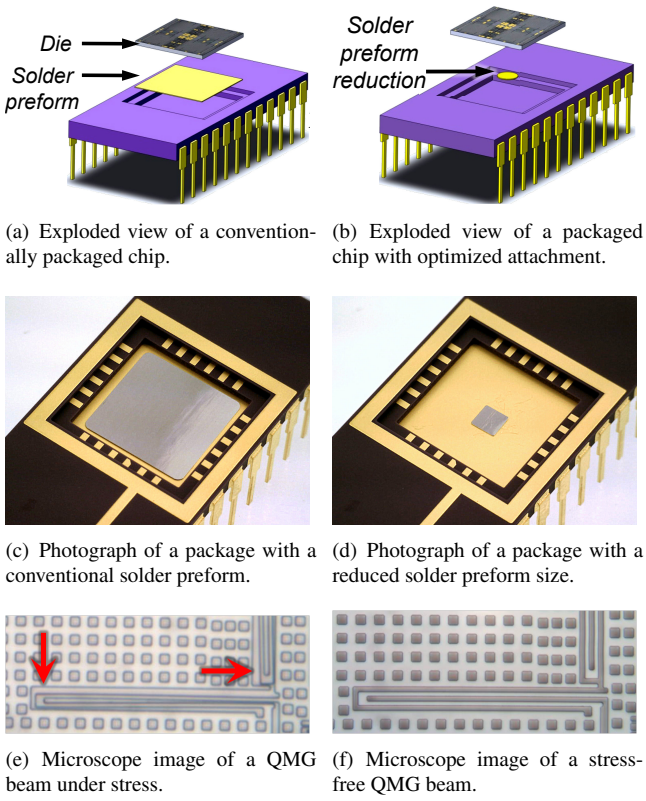

(a) Exploded view of a conventionally packaged chip.

(b) Exploded view of a packaged chip with optimized attachment.

(c) Photograph of a package with a conventional solder preform.

(d) Photograph of a package with a reduced solder preform size.

(e) Microscope image of a QMG beam under stress.

(f) Microscope image of a stress-free QMG beam.

Figure 4: Stress-free die attachment enabled by anchor size minimization.

weight applied on the anchored outer die frame to generate a force of no more than 1 N and obtain a void-free bond. Upon placement of components, the stack was heated above the gold-tin eutectic melting temperature of above 280 °C for solder reflow, and cooled down for solder solidification and resulting die bonding. To ensure high thermal conductivity, the temperature ramp up was performed in a partial vacuum (0.5 Torr), since conductivity is a function of temperature. Once the die was attached, it was wire-bonded and tested.

As an option, low pressure nitrogen gas can be introduced to provide better heat transfer. For complete void elimination, it is also possible to introduce high pressure (above 750 Torr) inside the chamber once the solder preform is melted and reached the liquid state [19]. According to the Boyle's Law, the high pressure collapses and reduces the size of void areas.

To verify the developed stress-free die attachment process, the packages with the quadruple mass gyroscope [14] dies were inspected using a microscope. Fig. 4(c) shows that the original die attachment eutectic reflow process is void free. However, inspection of the gyroscope suspension beams, Fig. 4(e), demonstrates significant bending due to the thermal expansion mismatch between the ceramic package and the silicon die. In contrast, the described process reduces packaging stresses by reducing a solder preform in size, Figs. 4(b) and 4(b). As shown in Figs. 4(d) and 4(f), anchor size minimization enables a stress-free device ready

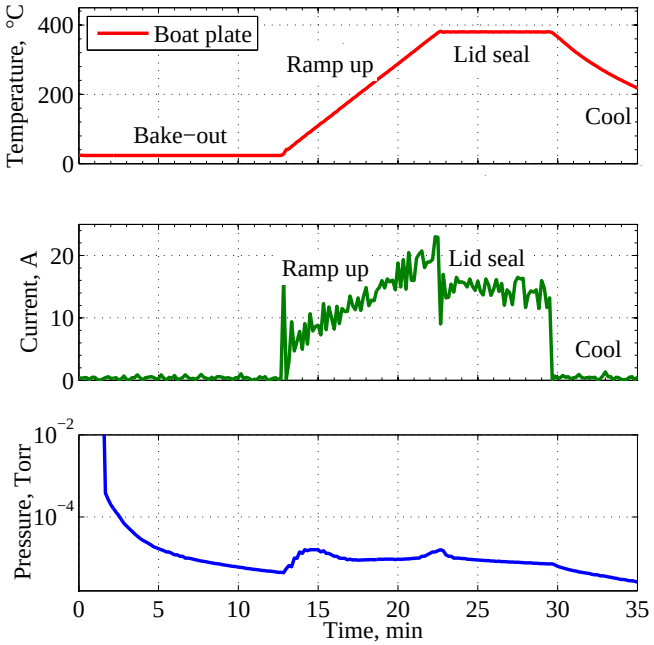

Figure 5: SST 3150 process parameters for moderate pressure level lid sealing without getters, including package temperature, plate current, and chamber pressure.

for testing and lid sealing. The measured frequency versus temperature for the vibratory modes of the vacuum packaged QMG also revealed that the dependency is linear with temperature coefficients close to silicon (below −31 ppm/°C).

4 Moderate-Level Vacuum Sealing

In this work the new packaging infrastructure has been tested for the hermetic lid sealing of the package cavity in a moderate pressure environment (0.5 Torr). The individual glass lids were obtained by dicing a 4" D263 glass wafer patterned with the gold metalized sealing squares of the cavity size. The glass material was chosen for its coefficient of thermal expansion close to that of the ceramic package. The preform frame of 80/20 gold-tin eutectic solder used as the bonding material was pre-attached to the package by using a hot soldering iron. This frame was tacked to the sealing square of the package without reflowing the solder.

Subsequently, a glass lid was mounted on the preform frame, and both the lid and package were placed in the vacuum furnace. In addition, weights were applied to the lid during the reflow process to ensure a void-free bond. The temperature profile of a sealing process, Fig. 5, was chosen to first bake out all the gas trapped in the plated metals, then seal the cavity by heating the system above the 280 °C eutectic temperature causing the preform to reflow, and finally cool down to solidify the frame and eventually bond the glass lid to the package. The result of the vacuum sealing process, Fig. 1, which shows the first completely packaged QMG prototype using an in-house facilities.

In order to verify the successful bond interface between

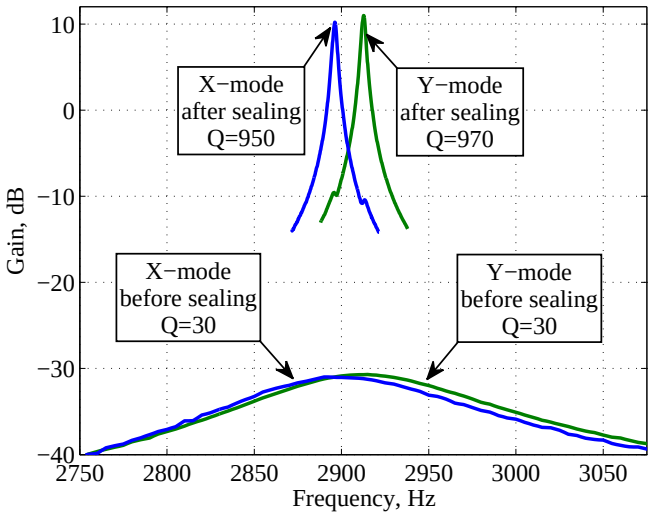

Figure 6: Frequency response of the 100 μm quadruple mass gyroscope packaged at moderate pressure level (0.5 Torr), showing both X- and Y-modes before and after sealing.

the lid and the ceramic package, Fig. 1, the stand-alone QMG prototype was experimentally characterized. The experimentally measured frequency responses of the anti-phase X- and Y-modes before and after vacuum sealing, Fig. 6, revealed Q-factors of 30 and 970, respectively.

The sealed cavity pressure of the stand-alone QMG prototype was estimated based on the Q-factor and pressure empiric relation, experimentally obtained for the quadruple mass gyroscope, Fig. 3. The cavity pressure corresponding to the measured Q-factor of 970 was determined to be approximately 0.5 Torr, which confirms the packaging procedure developed in-house for achieving stand-alone low pressure sealed resonant MEMS. As a future step, the next generation devices can be baked out up to 72 hours to achieve higher levels of vacuum.

5 High-Level Vacuum Sealing

Lid sealing with activated getter material enables and maintains a high vacuum (0.1 mTorr) inside the package cavity for the life of the device. Schematics of the lid sealing process flow is show in detail in Fig. 7. The getter thin film material is deposited on the glass or kovar lid (Fig. 1) prior to the hermetic sealing. Similar to the die attachment process, the preform frames of the same Au/Sn solder material are used for lid bonding. The process flow requires first to perform tacking of the solder frame to the package seal ring without reflowing it. This is a necessary step since the packages inside the SST 3150 tool are located upside down.

Once the solder frame is tacked to the package, the parts are placed into the vacuum chamber and the SST 3150 system is pumped down to approximately a μTorr pressure level. The two graphite locators are designed to fit up multiple DIP

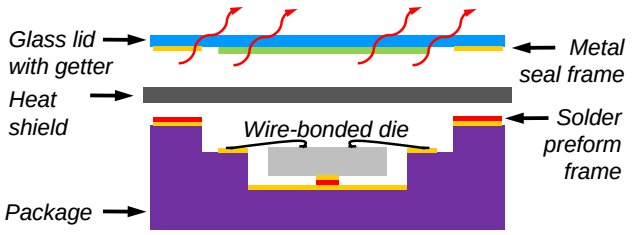

(a) Getter activation by heating the lid up to 450 °C in vacuum; the retractable heat shield protects the package from solder reflow.

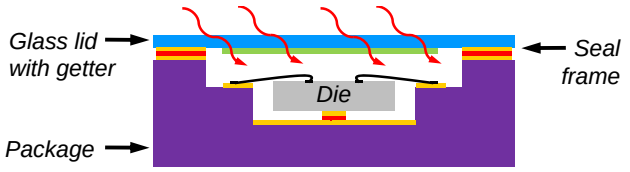

(b) Lid sealing by solder reflow at temperature above the melting point.

Figure 7: Process flow for lid sealing using getters.

packages with 24 pins. The "boat" graphite locator plate is stationary and doesn't move during the process. The purpose of the "boat" plate is to hold glass or kovar lids in place. This graphite "boat" also serves as a controlled heat source when current is applied. The second "lift" plate holds ceramic packages, which are located upside down. This plate can move during the process to a certain height in order to control the separation between the packages and the lids.

To ensure low outgassing, the ceramic packages and lids are baked-out for several hours at above 200 °C, Fig. 8. Both graphite plates are kept at the close separation to provide an effective heat transfer from the "boat" (heat source) to the "lift" plate, Fig. 8. Once the bake-out is completed, the chamber is prepared for getter activation by lifting up the plate to ensure separation of the packages from the heat sources. The getter activation is required since it is passivated to avoid reaction with the ambient environment. Activation is done by heating the lid up to 425 °C for 20 minutes, Figs. 7(a) and 8, which causes activation of the gas absorbing getter film. Since temperatures above 425 °C can cause premature reflow of the Au/Sn solder preforms, the heat shields are used to reduce heat transfer from the lower graphite "boat" with lids to the upper graphite "boat" with the ceramic packages and attached preform frames, Fig. 7(a). Once getters are activated, the heat protective shields are retracted and the plates are in contact, which allows to perform lid sealing by applying temperatures above the melting point and reflowing the Au/Sn eutectic solder. Fig. 8 shows the sample thermal profile of the high vacuum sealing process. Similar to the die attachment process, a void-free bond is achieved by applying cylinder weights to the packages during the reflow and solidification.

The resulting Q-factor of a stand-alone QMG prototype was investigated using ring-down tests. The time-domain amplitude decays of X- and Y-modes were fitted with exponential decays to extract time constants τ of 172 s and 174 s, respectively, Fig. 9. The Q-factors were calculated

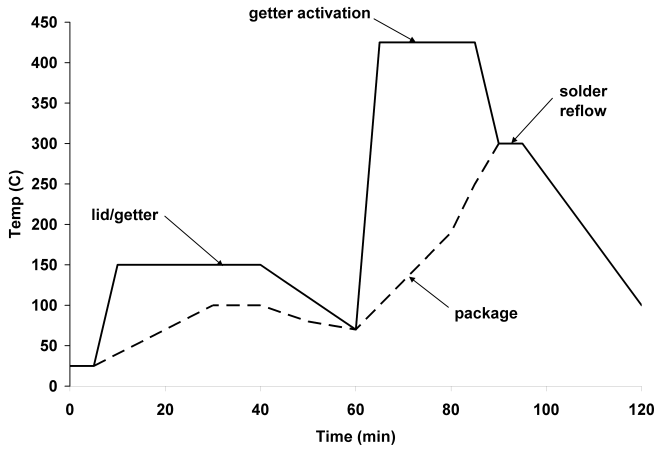

Figure 8: SST 3150 sample thermal profile for high vacuum lid sealing with getter activation, including package and lid temperatures [6].

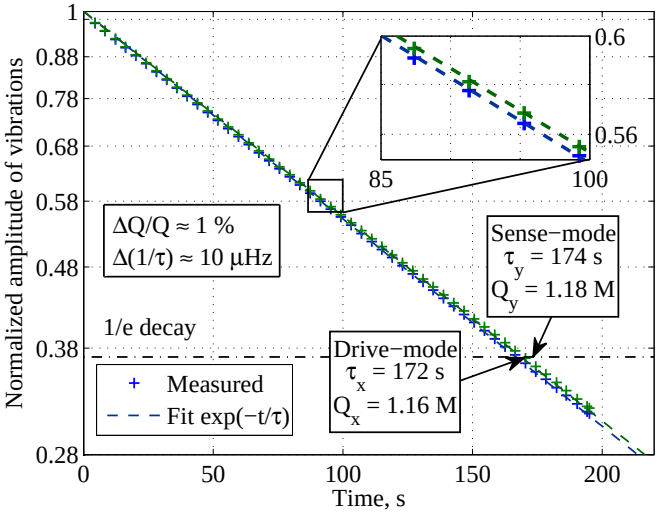

Figure 9: Experimental characterization of the packaged QMG using ring-down tests, revealing closely matched X- and Y-mode Q-factors of 1.17 million ±0.85%.

according to $Q = \pi f_n \tau$, with natural frequencies f_n of 2.2 kHz, Fig. 9. Exponential fits revealed identical drive- and sense-mode Q-factors of 1.17 million with $\Delta Q/Q$ variation of 1% before tuning or compensation, confirming the complete structural symmetry. The measured Q value is within 90% of the 1.3 million thermoelastic limit estimated by finite element modeling for the QMG design [14]. As shown in [15], the ultra-high Q-factor translates into the fundamental mechanical-thermal resolution limit of $10^{-4}\,^{\circ}/\sqrt{\text{hr}}$ for a zero frequency mismatch.

6 Conclusions

We developed and demonstrated the capabilities of the in-house versatile packaging infrastructure for both high and moderate-level vacuum sealing of resonant MEMS. Prototypes of 100 μm silicon-on-insulator quadruple mass

gyroscopes with optimized, high-Q design, were packaged using the developed process with and without getters. Experimental characterization of stand-alone packaged devices with no getters resulted in a stable quality factors of 1000 (corresponding to approximately 0.5 Torr vacuum level), while devices sealed with getter activation demonstrated Q-factors of approximately 1.2 million (below 0.1 mTorr level inside the package). These efforts effectively allowed to reach levels of pressure required for reaching the performance of inertial-grade MEMS gyroscopes.

Acknowledgment

The work was supported by the DARPA/SPAWAR under Contract N66001-12-C-4035. Igor P. Prikhodko and Brenton R. Simon contributed equally to this work. Authors would like to thank Dr. Flavio Heer of Zurich Instruments AG as well as David Muhs and Pierino Zappella of SST International. The devices were designed and tested at the MicroSystems Laboratory, UC Irvine.

References

[1] V.B. Braginsky, V.P. Mitrofanov, and V.I. Panov. *Systems with small dissipation*. Univ. Chicago Press, Chicago, IL, 1985.

[2] F. Ayazi. Multi-DOF inertial MEMS: From gaming to dead reckoning. In *Proc. of Solid-State Sensors, Actuators and Microsystems Conference (Transducers 2011)*, pages 2805–2808, Beijing, China, June 2011.

[3] B. Chaumet, B. Leverrier, C. Rougeot, and S. Bouyat. A new silicon tuning fork gyroscope for aerospace applications. In *Proc. of Symposium Gyro Technology*, pages 1.1–1.13, Karlsruhe, Germany, 2009.

[4] Z.X. Hu, B.J. Gallacher, J.S. Burdess, C.P. Fell, and K. Townsend. Precision mode matching of MEMS gyroscope by feedback control. In *Proc. of IEEE Sensors Conference*, pages 16–19, October 2011.

[5] B. Johnson, Eugen Cabuz, Howard French, and Ryan Supino. Development of a MEMS gyroscope for northfinding applications. In *Proc. of IEEE/ION Position, Location and Navigation Symposium (PLANS 2010)*, pages 168–170, Indian Wells/Palm Springs, CA, May 3–6, 2010.

[6] David Muhs and Paul Barnes. Controlling vacuum levels in discrete MEMS packages. In *Proc. of IMAPS International Conference and Exhibition on Device Packaging (DPC 2006)*, Phoenix, Arizona, March 20–23, 2006.

[7] I.P Prikhodko, S.A. Zotov, A.A. Trusov, and A.M. Shkel. Sub-degree-per-hour silicon MEMS rate sensor with 1 million Q-factor. In *Proc. of Solid-State Sensors, Actuators and Microsystems Conference (Transducers 2011)*, pages 2809–2812, Beijing, China, June 5–9, 2011.

[8] H. Rodjegard, D. Sandstrom, P. Pelin, N. Hedenstierna, D. Eckerbert, and G.I. Andersson. A digitally controlled MEMS gyroscope with 3.2 deg/hr stability. In *Proc. of Solid-State Sensors, Actuators and Microsystems Conference (Transducers 2005)*, volume 1, pages 535–538, 2005.

[9] S.G. Saraswathy, J. Geen, and J. Chang. High performance gyro with fast startup time, high range, wide bandwidth, low noise and excellent vibration immunity. In *Proc. of IEEE/ION Position, Location and Navigation Symposium (PLANS 2012)*, pages 20–23, Myrtle Beach, SC, April 23–26, 2012.

[10] Adam R. Schofield. *Design Algorithms and Trade-offs for Micromachined Vibratory Gyroscopes with Multi-Degree of Freedom Sense Modes*. PhD thesis, University of California, Irvine, CA, 2009.

[11] A.R. Schofield, A.A. Trusov, and A.M. Shkel. Versatile vacuum packaging for experimental study of resonant mems. In *Proc. of IEEE Micro Electro Mechanical Systems Conference (MEMS 2010)*, pages 516–519, Hong Kong S.A.R., China, January 24–28, 2010.

[12] K. Shcheglov, S. Orlov, J.C. Ha, and K. Ezal. Breakthrough and challenges of C-SWAP technology development. In *Proc. of JSDE/ION Joint Navigation Conference (JNC 2012)*, June 12–15, 2012.

[13] E. Tatar, S.E. Alper, and T. Akin. Quadrature-error compensation and corresponding effects on the performance of fully decoupled MEMS gyroscopes. *IEEE/ASME Journal of Microelectromechanical Systems*, 21(3):656–667, 2012.

[14] A.A. Trusov, I.P. Prikhodko, S.A. Zotov, and A.M. Shkel. Low-dissipation silicon tuning fork gyroscopes for rate and whole angle measurements. *IEEE Sensors Journal*, 11(11):2763–2770, November 2011.

[15] Alexander A. Trusov, Adam R. Schofield, and Andrei M. Shkel. Micromachined rate gyroscope architecture with ultra-high quality factor and improved mode ordering. *Sensors and Actuators, A: Physical*, 165(1):26–34, January 2011.

[16] Alexander A. Trusov, Adam R. Schofield, and Andrei M. Shkel. Micromachined tuning fork gyroscopes with ultra-high sensitivity and shock rejection, US patent 8322213, December 2012.

[17] M. Weinberg, J. Connelly, A. Kourepenis, and D. Sargent. Microelectromechanical instrument and systems development at the charles stark draper laboratory, inc. In *Proc. of AIAA/IEEE Digital Avionics Systems Conference (DASC)*, volume 2, pages 8.5–33–8.5–40, October 1997.

[18] M.F. Zaman, A. Sharma, Zhili Hao, and F. Ayazi. A mode-matched silicon-yaw tuning-fork gyroscope with subdegree-per-hour allan deviation bias instability. *IEEE/ASME Journal of Microelectromechanical Systems*, 17(6):1526–1536, December 2008.

[19] Pierino I. Zappella, Paul W. Barnes, David Muhs, and Bruce Wilson. RF/microwave die attach of gallium nitride devices achieving less than 1% voiding in a flux-free environment. In *Proc. of 45th International Symposium on Microelectronics (IMAPS 2012)*, San Diego, CA, September 9–13, 2012.

[20] S.A. Zotov, I.P Prikhodko, A.A. Trusov, and A.M. Shkel. Frequency modulation based angular rate sensor. In *Proc. of IEEE Micro Electro Mechanical Systems Conference (MEMS 2011)*, pages 577–580, Cancun, Mexico, January 23–27, 2011.

[21] S.A. Zotov, A.A. Trusov, and A.M. Shkel. High-range angular rate sensor based on mechanical frequency modulation. *IEEE/ASME Journal of Microelectromechanical Systems*, 21(2):398–405, April 2012.